On the Performance of Massive MIMO-NOMA Networks with Dual-Polarized Antenna Array

Arthur Sousa de Sena*, Daniel Benevides da Costa*, Zhiguo Ding†, and Pedro H. J. Nardelli‡
*Federal University of Ceará, Brazil
†The University of Manchester, UK
‡Lappeenranta University of Technology, Finland
Emails: arthurss@alu.ufc.br, danielbcosta@ieee.org, zhiguo.ding@manchester.ac.uk, pedro.nardelli@lut.fi

***Abstract*—This paper investigates the performance of multi-cluster multi-user massive multiple-input multiple-output (MIMO) networks with non-orthogonal multiple access (NOMA) and a dual-polarized antenna array. Considering the downlink mode in which a single base station communicates with multiple users, a precoder design is proposed with the aim to maximize the number of user groups that are simultaneously served within a cluster. A closed-form expression for the outage probability is derived, based on which an asymptotic analysis is carried out and the diversity gain is determined. Moreover, the outage sum-rate is also examined. Representative numerical examples are presented along with insightful discussions. Our results show that the proposed dual-polarized MIMO-NOMA design outperforms conventional single-polarized systems, even for high cross-polar interference.**

***Index Terms*—Non-orthogonal multiple access (NOMA), massive MIMO, multi-polarized antennas.**

I. Introduction

Non-orthogonal multiple access (NOMA) has arisen as an essential enabling technique for the fifth generation (5G) of wireless communications. It has the capability of increasing the spectral efficiency and, at the same time, to reduce the system latency. Briefly speaking, a base station (BS) superposes the messages of each user through superposition coding by assigning distinct power allocation coefficients and, at the receiver side, each user recovers its message by employing successive interference cancellation (SIC) technique. Due to the potential improvements that it achieves, NOMA was included in the 3rd generation partnership project (3GPP) long-term evolution advanced (LTE-A) Release-13 under the name of multi-user superposed transmission (MUST) and, more recently, in the 3GPP Release-14, where fifteen NOMA uplink schemes were proposed [1].

Massive multiple-input multiple-output (MIMO) is another enabling technology for 5G that can boost the system capacity by multiplexing multiple users through spatial domain. In combination with NOMA, massive MIMO systems can provide even higher spectral improvements that can remarkably outperform traditional orthogonal multiple access (OMA) protocols [2], [3]. The performance gains achieved in MIMO systems are scaled with the increase in the number of antennas. However, if the antenna elements are not separated by at least half of the wavelength, the system performance is severely degraded [4], [5]. Due to this impairing characteristic, in practical massive MIMO implementations, the maximum number of antennas is limited. To alleviate this issue, several works have considered the installation of co-located orthogonal polarized antennas [4]–[6]. Such strategy enables the design of compact massive arrays with very low correlation between orthogonal antenna elements. In addition to the space efficiency, it has been shown that massive MIMO systems employing dual-polarization can outperform the single-polarized counterpart with the same number of antenna elements [4], [6]. With these benefits, multi-polarization in massive MIMO have become the standard choice for LTE-A deployments, and it is expected to be part of 5G and beyond [7]. The employment of polarized antennas in MIMO-NOMA was only considered in [8], in which a 3D triple-polarized beamforming scheme was proposed to reduce inter-beam interference.

Although there is an uncountable number of relevant works for MIMO-NOMA and multi-polarized MIMO separately, to the best of the authors' knowledge, an in-depth understanding of the combination of these two subjects has not been examined in the literature so far. Therefore, this paper aims to investigate the performance of multi-cluster multi-user dual-polarized massive MIMO-NOMA systems. Specifically, we adopt a dual-stage precoder that is designed based only on the slowly varying spatial correlation information of the channel and aims to maximize the number of user groups that are simultaneously served. A closed-form expression for the outage probability is derived, based on which the asymptotic analysis is carried out and the diversity gain is determined. Moreover, the outage sum-rate is also examined. Representative numerical examples are presented along with insightful discussions. Our results show that the proposed dual-polarized MIMO-NOMA design outperforms conventional single-polarized systems, even for high cross-polar interference.

Notation and Special Functions: Bold-faced lower-case letters represent vectors and upper-case letters denote matrices. The norm and the i-th element of a vector $\mathbf{a}$ are represented by $\|\mathbf{a}\|$ and $[\mathbf{a}]_i$, respectively. The notations $[\mathbf{A}]_{i,j}$ and $[\mathbf{A}]_{i,*}$ correspond the (i,j) entry and the i-th row of the matrix $\mathbf{A}$, respectively. The Hermitian transposition of a matrix $\mathbf{A}$ is donated by $\mathbf{A}^H$ and the trace by $\text{tr}\{\mathbf{A}\}$. $\mathbf{I}_M$ represents the identity matrix of dimension $M \times M$, and $\mathbf{0}_{M\times N}$ denotes the $M \times N$ matrix with all zero entries. In addition, $\otimes$ represents the Kronecker product, $E[\cdot]$ denotes expectation, $\Gamma(\cdot)$ is the Gamma function, and $\gamma(\cdot,\cdot)$ corresponds to the lower incomplete Gamma function.

II. System Model

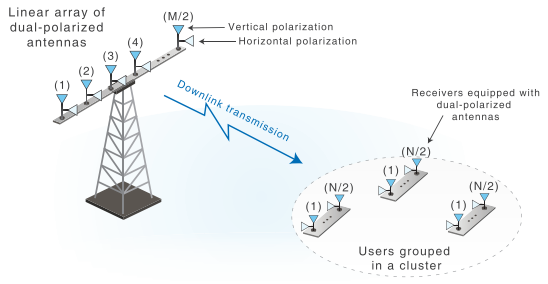

Fig. 1. System model.

Let a downlink transmit scenario in which a single BS communicates with multiple users, as illustrated in Fig. 1. The BS and the users are equipped, respectively, with $M/2$ and $N/2$ pairs of co-located dual-polarized antennas, with $M \gg N$. Due to the dual polarized structure, the total number of transmit and receive antennas are considered to be even. Furthermore, the users are assumed to be surrounded by local scatterers, forming K spatial clusters that follow the geometrical one-ring scattering model [3], [4]. Within each cluster k, there are L users that share the same spatial covariance matrix $\mathbf{R}_k \in \mathbb{C}^{M\times M}$. Besides, since each pair of polarized antennas are co-located, we assume equal covariance matrices for both polarizations.

With the given design and considerations, the correlated dual-polarized full channel matrix for the l-th user at the k-th cluster can be decomposed and expressed in the following block structure [4], [5]

$$\mathbf{H}_{k,l} = \begin{bmatrix} \mathbf{U}_k \mathbf{\Lambda}_k^{\frac{1}{2}} \mathbf{G}_{k,l}^{v\to v} & \sqrt{\chi}\mathbf{U}_k \mathbf{\Lambda}_k^{\frac{1}{2}} \mathbf{G}_{k,l}^{h\to v} \\ \sqrt{\chi}\mathbf{U}_k \mathbf{\Lambda}_k^{\frac{1}{2}} \mathbf{G}_{k,l}^{v\to h} & \mathbf{U}_k \mathbf{\Lambda}_k^{\frac{1}{2}} \mathbf{G}_{k,l}^{h\to h} \end{bmatrix} \in \mathbb{C}^{M\times N}, \tag{1}$$

with covariance matrix given by

$$\mathbf{R}_k = (\chi+1)\begin{bmatrix} \tilde{\mathbf{R}}_k & \mathbf{0} \\ \mathbf{0} & \tilde{\mathbf{R}}_k \end{bmatrix}, \tag{2}$$

where $\chi \in \{0,1\}$ stands for the inverse of the antennas' cross-polar discrimination parameter (XPD), $\tilde{\mathbf{R}}_k \in \mathbb{C}^{\frac{M}{2}\times\frac{M}{2}}$ represents the covariance matrix of rank r_k, corresponding to one polarization, $\mathbf{\Lambda}_k$ is an $r_k^\star \times r_k^\star$ diagonal matrix containing $r_k^\star$ nonzero eigenvalues of $\tilde{\mathbf{R}}_k$, with elements ordered in decreasing order, $\mathbf{U}_k \in \mathbb{C}^{\frac{M}{2}\times r_k^\star}$ denotes a matrix composed of eigenvectors of $\tilde{\mathbf{R}}_k$ corresponding to the nonzero eigenvalues, and $\mathbf{G}_{k,l}^{i\to j} \in \mathbb{C}^{r_k^\star \times \frac{N}{2}}$ is the channel matrix of the link between the i-th polarized transmitting antennas and the j-th polarized receiving antennas, $i,j \in \{v,h\}$, whose elements follow the complex Gaussian distribution with zero mean and unit variance. The letters h and v are used to indicate horizontal and vertical polarizations, respectively.

In order to enable the implementation of NOMA, similarly to the strategy presented in [3], the L users within a cluster are subdivided into G smaller groups of U users each, such that $L = UG$. Under this assumption, the superposition coding technique is applied to the data intended for users within a group. Thus, the transmitted data signal can be written as

$$\mathbf{x} = \sum_{k=1}^{K} \mathbf{B}_k \sum_{g=1}^{G} \mathbf{p}_{k,g} \sum_{u=1}^{U} \alpha_{k.g,u} s_{k,g,u}, \tag{3}$$

where $s_{k,g,u}$ and $\alpha_{k,g,u}$ are, respectively, the data symbol and the power coefficient for the u-th user in the g-th group of the k-th cluster. $\mathbf{B}_k \in \mathbb{C}^{M\times\bar{M}}$ is the preprocessing matrix which is designed based on the long-term channel state information, e.g., the covariance matrix $\mathbf{R}_k$, with $\bar{M}$ being a design parameter which defines the effective number of data streams that arrives at the receiver, and $\mathbf{p}_{k,g} \in \mathbb{C}^{\bar{M}\times 1}$ is a precoding vector for the g-th group.

III. Precoder Design and Signal Reception

Firstly, let us focus on the design of the preprocessing matrix $\mathbf{B}_k$. Our purpose is to extinguish the interfering signals coming from other clusters. Mathematically speaking, we must have $\mathbf{H}_{k,l}^H \mathbf{B}_{k'} \approx \mathbf{0}$, $\forall k \neq k'$. To accomplish this goal, the subspace spanned by the preprocessing matrix must be near-orthogonal (perfect orthogonality is achieved when $r_k^\star = r_k$) to the subspace spanned by the dominant eigenvectors of other clusters [9], which means that $\mathbf{B}_k$ must be built based on the null space of the dominant eigenmodes of interfering clusters. Then, we assume that $r_1^\star = r_2^\star = \ldots = r_K^\star = r^\star$, $r_1 = r_2 = \cdots = r_K = r$ and we define $\mathbf{U}_k^- = [\mathbf{U}_1, \cdots, \mathbf{U}_{k-1}, \mathbf{U}_{k+1}, \cdots, \mathbf{U}_K] \in \mathbb{C}^{\frac{M}{2}\times(K-1)r^\star}$.

Next, we apply the singular value decomposition (SVD) in $\mathbf{U}_k^-$ and express its left eigenvectors as $\mathbf{E}_k = [\mathbf{E}_k^{(1)}, \mathbf{E}_k^{(0)}]$, where $\mathbf{E}_k^{(0)} \in \mathbb{C}^{\frac{M}{2}\times\frac{M}{2}-(K-1)r^\star}$ represents the eigenvectors that correspond to the last $\frac{M}{2}-(K-1)r^\star$ vanishing eigenvalues of $\mathbf{U}_k^-$. Since $(\mathbf{E}_k^{(0)})^H \mathbf{U}_k^- = \mathbf{0}$, the projected channel that is orthogonal to the dominant $r^\star$ eigenmodes of the groups $k' \neq k$ can be defined as $\hat{\mathbf{H}}_{k,l} = (\mathbf{I}_2 \otimes \mathbf{E}_k^{(0)})^H \mathbf{H}_{k,l}$. Consequently, the covariance matrix of $\hat{\mathbf{H}}_{k,l}$ is given by $\hat{\mathbf{R}}_k = (\mathbf{I}_2 \otimes \mathbf{E}_k^{(0)})^H \mathbf{R}_k (\mathbf{I}_2 \otimes \mathbf{E}_k^{(0)})$, and the covariance matrix considering only one of the polarizations can be written as $\underline{\hat{\mathbf{R}}}_k = (\mathbf{E}_k^{(0)})^H \tilde{\mathbf{R}}_k \mathbf{E}_k^{(0)}$. By defining the left eigenvectors of $\underline{\hat{\mathbf{R}}}_k$ as $\mathbf{F}_k = [\mathbf{F}_k^{(1)}, \mathbf{F}_k^{(0)}]$, in which $\mathbf{F}_k^{(1)} \in \mathbb{C}^{\frac{M}{2}-(K-1)r^\star\times\frac{\bar{M}}{2}}$ consists of the first $\frac{\bar{M}}{2}$ columns of $\mathbf{F}_k$, the precoder design can be obtained as follows

$$\tilde{\mathbf{B}}_k = \mathbf{E}_k^{(0)} \mathbf{F}_k^{(1)} \in \mathbb{C}^{\frac{M}{2}\times\frac{\bar{M}}{2}}, \quad \mathbf{B}_k = \mathbf{I}_2 \otimes \tilde{\mathbf{B}}_k \in \mathbb{C}^{M\times\bar{M}}, \tag{4}$$

in which $K \leq \bar{M} \leq 2\left(\frac{M}{2} - (K-1)r^\star\right)$ and $\bar{M} \leq 2r^\star \leq 2r$.

It is important to highlight that $r^\star$ is a design parameter that should be adjusted based on how much inter-cluster interference is tolerable in the system. The closer the value of $r^\star$ gets to r, less inter-cluster interference the system will experience. However, as stated in [9], choosing $r^\star$ too large, e.g., $r^\star = r$, does not bring significant improvements. Instead, it will only force a reduction on the number of clusters that are simultaneously served. Therefore, the parameter $r^\star$ should be carefully chosen in order to attend the system requirements.

For the inner precoder, we assume that the BS has access only to the slow-fading covariance matrix $\tilde{\mathbf{R}}_k$. Thus, $\mathbf{p}_{k,g}$ is

designed in a way that it will not depend on the short-term channel state information. Also, the precoding vector aims to maximize the number of groups there are simultaneously served within a cluster. To this end, we choose to assign to each group a different antenna element so that a maximum of $\bar{M}$ parallel transmissions can be performed. More specifically, supposing that $G \leq \bar{M}$, the precoding vector is chosen as

$$\mathbf{p}_{k,g} = [\ \mathbf{0}_{1\times(g-1)}\ ,\ 1\ ,\ \mathbf{0}_{1\times(\bar{M}-g)}\ ]^T. \tag{5}$$

Note that, with the above precoder, the g-th antenna element is assigned to the g-th group.

A. Signal Reception

Considering that $\mathbf{B}_k$ completely removes the interference from other clusters, the u-th user at the g-th group of the k-th cluster observes the following

$$\mathbf{y}_{k,g,u} = \mathbf{H}_{k,g,u}^H \mathbf{B}_k \sum_{m=1}^{G} \mathbf{p}_{k,m} \sum_{n=1}^{U} \alpha_{k,m,n} s_{k,m,n} + \mathbf{n}_{k,g,u}. \tag{6}$$

where $\mathbf{n}_{k,g,u} \in \mathbb{C}^{N\times 1}$ is the noise vector with entries obeying a complex Gaussian distribution with zero-mean and variance σ_n^2.

Now, in order to eliminate the inter-group interference and recover the desired signal, a zero-forcing equalizer is adopted at the users side. Supposing that $N \geq \bar{M}$, the Moore-Penrose pseudo-inverse of the virtual channel $\bar{\mathbf{H}}_{k,g,u} = \mathbf{H}_{k,g,u}^H \mathbf{B}_k \in \mathbb{C}^{N\times\bar{M}}$ can be defined as $\bar{\mathbf{H}}_{k,g,u}^{\dagger} = (\bar{\mathbf{H}}_{k,g,u}^H \bar{\mathbf{H}}_{k,g,u})^{-1} \bar{\mathbf{H}}_{k,g,u}^H \in \mathbb{C}^{\bar{M}\times N}$. After multiplying (6) by $\bar{\mathbf{H}}_{k,g,u}^{\dagger}$, the interference is removed and the u-th user acquires a vector formed by the noisy version of the transmitted superimposed symbols. Given the precoder in (5), and, for simplicity, assuming that the number of groups is $G = \bar{M}$, the detected vector can be expressed as

$$\hat{\mathbf{s}}_{k,g,u} = \begin{bmatrix} \sum_{n=1}^{U} \alpha_{k,1,n} s_{k,1,n} \\ \vdots \\ \sum_{n=1}^{U} \alpha_{k,G,n} s_{k,G,n} \end{bmatrix} + \bar{\mathbf{H}}_{k,g,u}^{\dagger} \mathbf{n}_{k,g,u}. \tag{7}$$

One can see that each element of (7) belongs to a specific group. Therefore, the u-th user at the g-th group recovers its message from the g-th element of the received vector $\hat{\mathbf{s}}_{k,g,u}$.

IV. Performance Analysis

In this section, the performance of the proposed multi-polarized massive MIMO-NOMA system is evaluated. A closed-form expression for the outage probability is derived, based on which an asymptotic analysis at high signal-to-noise ratio (SNR) regime is carried out.

A. Signal-to-Interference-plus-Noise Ratio (SINR) Analysis

After the superimposed data symbol is recovered, the user employs SIC in order to retrieve its message. To successfully complete the SIC process, it is crucial to have knowledge about the ordering of users' effective gains. Therefore, it is assumed that the BS has complete access to the user ordering information. Moreover, it is considered that the effective channel gains are sorted out in increasing order of magnitude, meaning that the 1st user has the weakest gain and the U-th user has the strongest one. Under these assumptions, the SINR for the proposed dual-polarized system can be defined by the following lemma.

Lemma I: During the SIC process, the SINR of the data symbol intended for the i-th weaker user that is observed at the current u-th user in the g-th group of the k-th cluster is given by

$$\gamma_{k,g,u}^{i} = \frac{\zeta_{k,g,u}\alpha_{k,g,i}^2}{\zeta_{k,g,u}\mathcal{I}_i + \frac{1}{\rho}}, \qquad \text{for} \quad 1 \leq i \leq U. \tag{8}$$

where $\rho = \frac{1}{\sigma_n^2}$ denotes the transmit SNR, $\zeta_{k,g,u} = \frac{1}{\|[\bar{\mathbf{H}}_{k,g,u}^{\dagger}]_{g,*}\|^2}$ is the effective channel gain, and $\mathcal{I}_i$ corresponds to the power of interfering messages, being defined by

$$\mathcal{I}_i = \begin{cases} \sum_{j=i+1}^{U} \alpha_{k,g,j}^2, & \text{for} \quad 1 \leq i \leq u < U, \\ 0, & \text{for} \quad i = u = U, \end{cases} \tag{9}$$

Proof: Please, see Appendix A.

One can see that the interference factor defined in (9) reaches its maximum value when the first user, the weakest one, decodes its message. This is the expected since the first user does not decode messages from others, only its own, suffering interference from all the other users. On the other hand, assuming perfect SIC, the strongest user recovers its own message with zero interference.

B. Outage Probablity

The outage probability for the u-th user in the g-th group of the k-th cluster, denoted by $P_{k,g,u}^{\text{out}}$, can be defined as the probability of the message intended to the i-th user being received at the u-th user with a date rate less than the required target rate $\mathcal{R}_{k,g,i}$, $\forall\ 1 \leq i \leq u$, i.e.,

$$P_{k,g,u}^{\text{out}} = P[\log_2(1+\gamma_{k,g,u}^{i}) < \mathcal{R}_{k,g,i}], \quad \forall i = 1, \cdots u. \tag{10}$$

From (10), a closed-form expression for the outage probability of the proposed dual-polarized massive MIMO-NOMA system is derived next.

Proposition I: Assuming that the users are sorted out in increasing order based on their effective channel gains, the outage probability can be derived as

$$P_{k,g,u}^{\text{out}} = \mathcal{U}_u \sum_{n=0}^{U-u} (-1)^n\ (U-un) \times \frac{1}{u+n} \left[\frac{\gamma\left(\eta, (\chi+1)\beta_{k,g}\rho^{-1}\Upsilon_{k,g,u}\right)}{\Gamma(\eta)} \right]^{u+n}, \tag{11}$$

where $\mathcal{U}_u = U\ (U-1u-1)$, $\beta_{k,g} = [\mathbf{I}_2 \otimes (\tilde{\mathbf{B}}_k^H \tilde{\mathbf{R}}_k \tilde{\mathbf{B}}_k)^{-1}]_{g,g}$, $\Upsilon_{k,g,u} = \max\limits_{i\in[1,u]} \left\{ \frac{2^{\mathcal{R}_{k,g,i}}-1}{\alpha_{k,g,i}^2 - \mathcal{I}_i(2^{\mathcal{R}_{k,g,i}}-1)} \right\}$, and $\eta = \frac{N}{2} - \frac{\bar{M}}{2} + 1$.

Proof: Please, see Appendix B.

C. Asymptotic Analysis

In order to gain further insights from the derived expression, an asymptotic analysis is now performed.

Proposition II: When the transmit SNR goes to infinity, i.e., $\rho \to \infty$, the outage probability expression in (11) can be approximated by

$$P_{k,g,u}^{\text{out}} \approx \frac{1}{\rho^{\eta u}} \frac{\mathcal{U}_u}{u} \frac{[(\chi+1)\beta_{k,g}\Upsilon_{k,g,u}]^{\eta u}}{(\eta!)^u}, \tag{12}$$

which yields a diversity order at the u-th user of

$$\mathcal{D}_u = \left(\frac{N}{2} - \frac{\bar{M}}{2} + 1\right) u. \tag{13}$$

Proof: Please, see Appendix C.

From the asymptotic results, one can see that the system performance increases with the order of the users. This behavior is in fact expected, since the higher is the user order, the better is its channel condition.

V. Numerical and Simulation Results

In this section, the performance of the proposed dual-polarized massive MIMO-NOMA system is investigated. Otherwise stated, the BS is equipped with $M/2 = 50$ pairs of collocated horizontally and vertically polarized antennas arranged in a uniform linear array, where each pair of elements is separated by half of the wavelength, i.e., $\lambda/2$. For comparison purposes, single-polarized systems are equipped with the same number M of transmit antennas, with elements being also separated by $\lambda/2$. Without loss of generality, we consider the existence of $K = 4$ spatial clusters, each one containing $L = 6$ users that are subdivided into $G = 2$ groups of $U = 3$ users each, and we adjust the BS azimuth inclination angle to the direction of the cluster of interest, providing maximum array gain. The power allocation coefficients of Users 1, 2 and 3 are set to $\alpha_1 = 0.63, \alpha_2 = 0.25, \alpha_3 = 0.12$, and the target rates to $\mathcal{R}_1 = \mathcal{R}_2 = 1.4, \mathcal{R}_3 = 4$ bits per channel use (BPCU), respectively. In addition, the number of effective data streams is set to $\bar{M} = 4$. All simulation results are generated through 2×10^5 Monte Carlo iterations, and a perfect agreement with the analytical ones is observed in all the plots.

Fig. 2 plots the outage probability versus transmit SNR. As it can be realized, the system performance gets worse as χ gets higher. However, it is interesting to note that, even with a high inverse XPD value, the dual-polarized system shows superior performance than the single-polarized one, such that, for $\chi = 0.5$, the dual-polarized user with better channel conditions requires approximately 3dB less than for the single case to achieve the same level of outage. Fig. 3 shows the exact outage probability curves along with their respective asymptotic behaviors, in which a perfect agreement at high SNR regions is observed among the curves. This validates the analytical derivation of Proposition II.

In Fig. 4, the outage sum-rate, obtained as $\sum_{n=1}^{U}(1 - P_{k,g,n}^{\text{out}})\mathcal{R}_{k,g,n}$, is investigated. As can be observed, antenna polarization can provide significant spectral improvements. For instance, by employing $N = 4$ receive antennas at a SNR

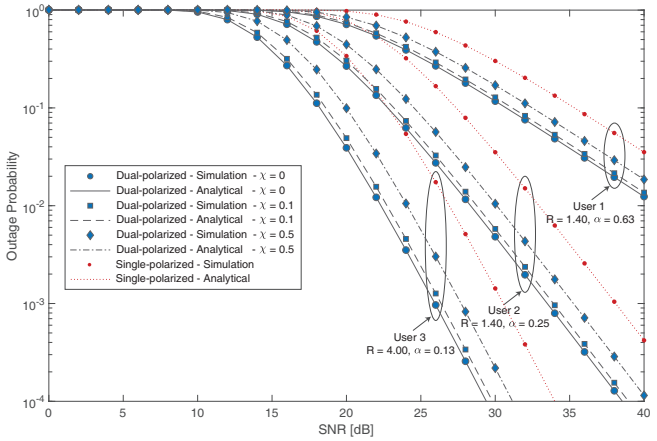

Fig. 2. Outage probability versus transmit SNR for dual-polarized massive MIMO-NOMA system ($N = 4$).

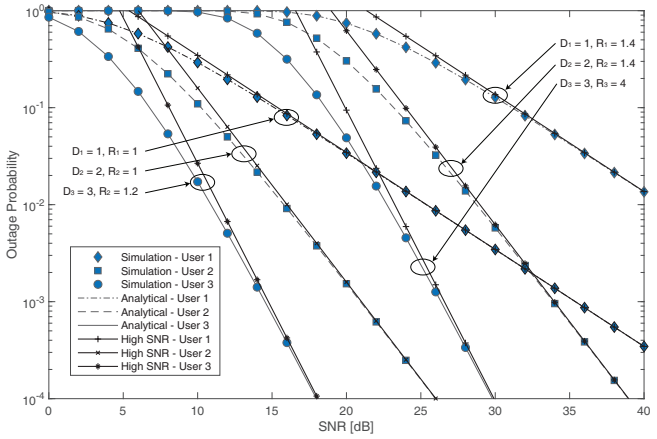

Fig. 3. Exact and asymptotic outage probability curves for dual-polarized massive MIMO-NOMA system ($N = 4$ and $\chi = 0.1$).

of 18dB, the dual-polarized system achieves a throughput of 4.3 BPCU. This is almost three times greater than that of the single-polarized system with the same number of antennas. Lastly, Fig. 5 compares the outage sum-rate performance of the dual-polarized MIMO-NOMA system with the single-polarized OMA and NOMA cases. One can observe that the dual-polarized NOMA systems outperform the classic OMA scheme in almost all considered SNR range, while the single-polarized MIMO-NOMA case becomes better only for SNR values higher than 19dB, which demonstrates again the benefits of polarization.

VI. Conclusions

In this work, we have investigated the application of a dual-polarized antenna array in a massive MIMO-NOMA setup. A precoder design was proposed and investigated, and a detailed analytical analysis in terms of outage probability and outage/ergodic sum-rate was provided. Our results showed that the proposed dual-polarized MIMO-NOMA design outperforms conventional single-polarized systems, even for high cross-polar interference, corroborating the fact that polarization has great potential to bring significant improvements to conventional massive MIMO-NOMA deployments.

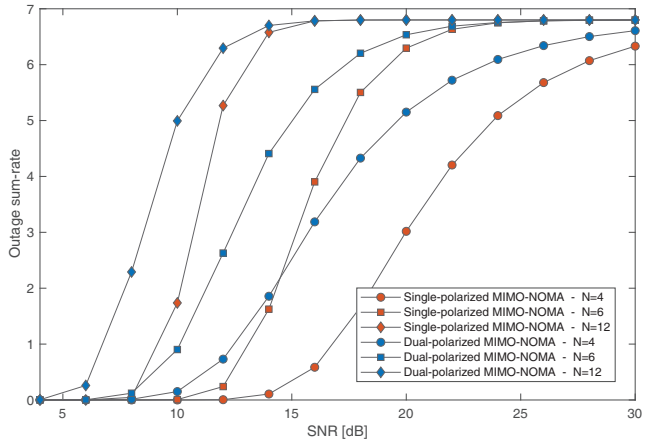

Fig. 4. Outage sum-rate for single-polarized and dual-polarized MIMO-NOMA systems ($\chi = 0.1$).

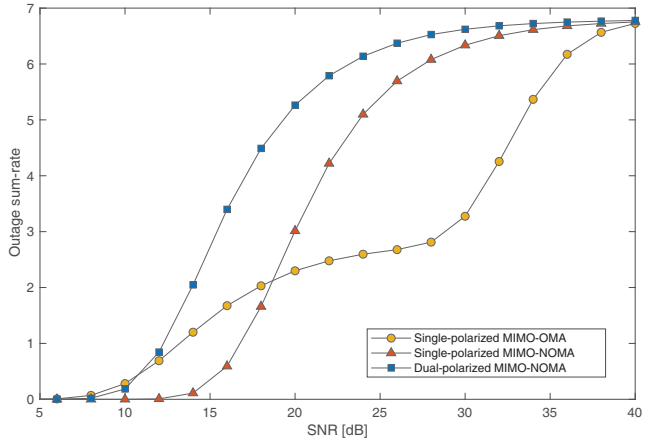

Fig. 5. Outage sum-rate curves for single-polarized MIMO-OMA/MIMO-NOMA systems and dual-polarized MIMO-NOMA system ($N = 4$ and $\chi = 0.001$).

Appendix A
Proof of Lemma I

To successfully apply SIC, the effective channel gains of the users within a group must be ordered. Then, assuming that $\zeta_{k,g,1} < \zeta_{k,g,2} < \cdots < \zeta_{k,g,U}$, the message intended to the i-th weaker user that is observed at the u-th user within the g-th group of the k-th cluster is decoded with the following SNR

$$\gamma^i_{k,g,u} = \frac{E[|\alpha_{k,g,i} s_{k,g,i}|^2]}{E\left[\sum_{j=i+1}^{U} |\alpha_{k,g,j} s_{k,g,j}|^2\right] + E[|[\bar{\mathbf{H}}^{\dagger}_{k,g,u} \mathbf{n}_{k,g,u}]_g|^2]}. \tag{A-1}$$

Knowing that

$$E[\|\bar{\mathbf{H}}^{\dagger}_{k,g,u} \mathbf{n}_{k,g,u}\|^2] = \sigma_n^2 E[\mathrm{tr}\{\bar{\mathbf{H}}^{\dagger}_{k,g,u} \bar{\mathbf{H}}^{\dagger H}_{k,g,u}\}], \tag{A-2}$$

and since only the g-th element of $\hat{\mathbf{s}}_{k,g,u}$ is desired, the second term in the denominator of (A-1) can be simplified to

$$E[|[\bar{\mathbf{H}}^{\dagger}_{k,g,u} \mathbf{n}_{k,g,u}]_g|^2] = \sigma_n^2 \|[\bar{\mathbf{H}}^{\dagger}_{k,g,u}]_{g,*}\|^2, \tag{A-3}$$

Now, by substituting (A-3) in (A-1) and defining the transmit SNR as $\rho = \frac{1}{\sigma_n^2}$, we get

$$\gamma^i_{k,g,u} = \frac{\frac{1}{\|[\bar{\mathbf{H}}^{\dagger}_{k,g,u}]_{g,*}\|^2} \alpha^2_{k,g,i}}{\sum_{j=i+1}^{U} \frac{1}{\|[\bar{\mathbf{H}}^{\dagger}_{k,g,u}]_{g,*}\|^2} \alpha^2_{k,g,j} + \frac{1}{\rho}}, \quad 1 \le i \le u < U. \tag{A-4}$$

From (A-4), the effective channel gain can be defined as $\zeta_{k,g,u} = \frac{1}{\|[\bar{\mathbf{H}}^{\dagger}_{k,g,u}]_{g,*}\|^2}$. In addition, it can be noticed that when $i = u = U$, there is no interfering messages and the first term of the denominator in (A-4) equals zero. Then, the following is defined

$$\mathcal{I}_i = \begin{cases} \sum_{j=i+1}^{U} \alpha^2_{k,g,j}, & \text{for} \quad 1 \le i \le u < U, \\ 0, & \text{for} \quad i = u = U. \end{cases} \tag{A-5}$$

Finally, by replacing $\zeta_{k,g,u}$ and (A-5) in (A-4), the SINR expression becomes

$$\gamma^i_{k,g,u} = \frac{\zeta_{k,g,u} \alpha^2_{k,g,i}}{\zeta_{k,g,u} \mathcal{I}_i + \frac{1}{\rho}}, \quad \text{for} \quad 1 \le i \le U, \tag{A-6}$$

which concludes the proof of Lemma 1.

Appendix B
Proof of Proposition I

We first simplify (10) as following

$$P^{\text{out}}_{k,g,u} = P\left[\zeta_{k,g,u} < \frac{1}{\rho} \frac{2^{\mathcal{R}_{k,g,i}} - 1}{\alpha^2_{k,g,i} - \mathcal{I}_i(2^{\mathcal{R}_{k,g,i}} - 1)}\right]. \tag{B-1}$$

Let $\Upsilon_{k,g,u} = \max_{i \in [1,u]} \left\{ \frac{2^{\mathcal{R}_{k,g,i}} - 1}{\alpha^2_{k,g,i} - \mathcal{I}_i(2^{\mathcal{R}_{k,g,i}} - 1)} \right\}$. Then, (B-1) becomes

$$P^{\text{out}}_{k,g,u} = P\left[\zeta_{k,g,u} < \rho^{-1} \Upsilon_{k,g,u}\right]. \tag{B-2}$$

Note that (B-2) represents the cumulative distribution function (CDF) of the effective channel gain. As established in Lemma I, the effective channel gain for the u-th user is given by $\zeta_{k,g,u} = \frac{1}{\|[\bar{\mathbf{H}}^{\dagger}_{k,g,u}]_{g,*}\|^2}$. This value corresponds to the inverse g-th diagonal element of the covariance matrix $\mathbf{\Xi}_{k,g,u} = \bar{\mathbf{H}}^{\dagger}_{k,g,u} \bar{\mathbf{H}}^{\dagger H}_{k,g,u}$. Thus, with the purpose of determining the main diagonal marginal distribution of $\mathbf{\Xi}_{k,g,u}$, we perform the following expansion

$$\begin{aligned} \mathbf{\Xi}_{k,g,u} &= (\bar{\mathbf{H}}^H_{k,g,u} \bar{\mathbf{H}}_{k,g,u})^{-1} \bar{\mathbf{H}}^H_{k,g,u} \bar{\mathbf{H}}_{k,g,u} (\bar{\mathbf{H}}^H_{k,g,u} \bar{\mathbf{H}}_{k,g,u})^{-1} \\ &= \frac{\mathbf{I}_2 \otimes (\tilde{\mathbf{B}}^H_k \tilde{\mathbf{R}}_k \tilde{\mathbf{B}}_k)^{-1}}{\chi + 1} = \frac{\mathbf{I}_2 \otimes \tilde{\mathbf{W}}^{-1}_k}{\chi + 1} \end{aligned} \tag{B-3}$$

where $\tilde{\mathbf{W}}_k = \tilde{\mathbf{B}}^H_k \tilde{\mathbf{R}}_k \tilde{\mathbf{B}}_k$. Given that the matrices $\mathbf{G}^{i \to j}_{k,l}$ have complex Gaussian entries, the resulting matrix $\mathbf{G}^{i \to j}_{k,l} (\mathbf{G}^{i \to j}_{k,l})^H$ is complex Wishart distributed. As a consequence, the matrix $\tilde{\mathbf{W}}_k$ also follows the Wishart distribution and, in this way, $\tilde{\mathbf{W}}^{-1}_k$ is inverse Wishart distributed with $\frac{N}{2}$ degrees of freedom and covariance matrix $(\tilde{\mathbf{B}}^H_k \tilde{\mathbf{R}}_k \tilde{\mathbf{B}}_k)^{-1}$ [3], [10].

At this point, we already know the distribution of $\tilde{\mathbf{W}}^{-1}_k$. However, we are interested in the distribution of the inverse

$$P_{k,g,u}^{\text{out}} = \mathcal{U}_u \sum_{n=0}^{U-u} (-1)^n (U-un) \frac{(\chi+1)^\eta \beta_{k,g}^\eta}{\Gamma(\eta)^{u+n}} \int_0^{\rho^{-1}\Upsilon_{k,g,u}} x^{\eta-1} e^{-(\chi+1)\beta_{k,g}x} \gamma\left(\eta, (\chi+1)\beta_{k,g}x\right)^{u-1+n} dx$$
$$= \mathcal{U}_u \sum_{n=0}^{U-u} (-1)^n (U-un) \frac{1}{u+n} \left[\frac{\gamma\left(\eta, (\chi+1)\beta_{k,g}\rho^{-1}\Upsilon_{k,g,u}\right)}{\Gamma(\eta)}\right]^{u+n}. \quad \text{(B-9)}$$

$$\frac{\gamma\left(\eta, (\chi+1)\beta_{k,g}\rho^{-1}\Upsilon_{k,g,u}\right)}{\Gamma(\eta)} = 1 - e^{-(\chi+1)\beta_{k,g}\rho^{-1}\Upsilon_{k,g,u}} \sum_{m=0}^{\eta-1} \frac{[(\chi+1)\beta_{k,g}\rho^{-1}\Upsilon_{k,g,u}]^m}{m!} < \frac{[(\chi+1)\beta_{k,g}\rho^{-1}\Upsilon_{k,g,u}]^\eta}{\eta!}. \quad \text{(C-1)}$$

of the main diagonal elements of $\mathbf{\Xi}_{k,g,u}$. The marginal distribution of the main diagonal of an inverse Wishart matrix also follows the inverse Wishart distribution and it is equivalent to the univariate inverse Gamma distribution [10]. Thus, the inverse of the diagonal elements of $\mathbf{I}_2 \otimes \tilde{\mathbf{W}}_k^{-1}$ follows the Gamma distribution. Consequently, considering the unordered case, the CDF for the inverse of diagonal elements of $\mathbf{\Xi}_{k,g,u}$ is given by [11]

$$F(x) = \frac{\gamma\left(\eta, (\chi+1)\beta_{k,g}x\right)}{\Gamma(\eta)}, \quad \text{(B-4)}$$

and the corresponding probability density function (PDF) can be written as

$$f(x) = \frac{(\chi+1)^\eta \beta_{k,g}^\eta x^{\eta-1} e^{-(\chi+1)\beta_{k,g}x}}{\Gamma(\eta)}, \quad \text{(B-5)}$$

where $\eta = \frac{N}{2} - \frac{\bar{M}}{2} + 1$ and $\beta_{k,g} = [\mathbf{W}_k^{-1}]_{g,g} = [\mathbf{I}_2 \otimes (\tilde{\mathbf{B}}_k^H \tilde{\mathbf{R}}_k \tilde{\mathbf{B}}_k)^{-1}]_{g,g}$. For the ordered case, we can consider the effective channel gain $\zeta_{k,g,u}$ as the u-th order statistic. Therefore, the PDF for the u-th ordered channel gain can be obtained as [10]

$$f_{\zeta_{k,g,u}}(x) = U\left(U-1u-1\right) f(x) F(x)^{u-1} (1-F(x))^{U-u}. \quad \text{(B-6)}$$

For convenience, we rewrite the term $(1-F(x))^{U-u}$ as $\sum_{n=0}^{U-u}(-1)^n (U-un) F(x)^n$ and define $\mathcal{U}_u = U\left(U-1u-1\right)$. Then, (B-6) becomes

$$f_{\zeta_{k,g,u}}(x) = \mathcal{U}_u \sum_{n=0}^{U-u} (-1)^n (U-un) \frac{(\chi+1)^\eta \beta_{k,g}^\eta}{\Gamma(\eta)^{u+n}} \times x^{\eta-1} e^{-(\chi+1)\beta_{k,g}x} \gamma\left(\eta, (\chi+1)\beta_{k,g}x\right)^{u-1+n}. \quad \text{(B-7)}$$

Finally, by integrating (B-7), a closed-form expression for the outage probability of the u-th user in the g-th group of the k-cluster can de derived as in (B-9), shown at the top of the page. This completes the proof.

Appendix C
Proof of Proposition II

Since $\eta = \frac{N}{2} - \frac{\bar{M}}{2} + 1$, and considering that $\frac{N}{2} \geq \frac{\bar{M}}{2}$, η assumes only positive integer values. Then, a series representation for this special case can be applied to simplify the Gamma function presented in (11) as in (C-1) [12], shown at the top of this page. Thus, the high-SNR outage probability approximation for the proposed dual-polarized system can be obtained by replacing (C-1) in (11), which results in

$$P_{k,g,u}^{\text{out}} \approx \mathcal{U}_u \sum_{n=0}^{U-u} (-1)^n (U-un) \times \frac{1}{u+n} \frac{[(\chi+1)\beta_{k,g}\rho^{-1}\Upsilon_{k,g,u}]^{\eta(u+n)}}{(\eta!)^{u+n}} \approx \frac{1}{\rho^{\eta u}} \frac{\mathcal{U}_u}{u} \frac{[(\chi+1)\beta_{k,g}\Upsilon_{k,g,u}]^{\eta u}}{(\eta!)^u}, \quad \text{(C-2)}$$

and the diversity order reached by the u-th user is

$$\mathcal{D}_u = \eta u = \left(\frac{N}{2} - \frac{\bar{M}}{2} + 1\right) u. \quad \text{(C-3)}$$

The proof is complete.

References

[1] Y. C. *et al.*, "Toward the standardization of non-orthogonal multiple access for next generation wireless networks," *IEEE Commu. Mag.*, vol. 56, no. 3, pp. 19–27, Mar. 2018.

[2] Z. Ding, F. Adachi, and H. V. Poor, "The application of MIMO to non-orthogonal multiple access," *IEEE Trans. Wireless Commun.*, vol. 15, no. 1, pp. 537–552, Jan. 2016.

[3] Z. Ding and V. Poor, "Design of massive-MIMO-NOMA with limited feedback," *IEEE Signal Proces. Let.*, vol. 23, no. 5, May 2016.

[4] J. Park and B. Clerckx, "Multi-user linear precoding for multi-polarized massive MIMO system under imperfect CSIT," *IEEE Trans. Wireless Commun.*, vol. 14, no. 05, May 2015.

[5] T. Kim, B. Clerckx, D. J. Love, and S. J. Kim, "Limited feedback beamforming systems for dual-polarized MIMO channels," *IEEE Trans. Wireless Commun.*, vol. 9, no. 11, Nov. 2010.

[6] X. Cheng, Y. He, and M. Guizani, "3-D geometrical model for multi-polarized MIMO systems," *IEEE Access*, vol. 5, pp. 11 974–11 984, 2017.

[7] F. Zheng, Y. Chen, B. Pang, C. Liu, S. Wang, D. Fan, and J. Zhang, "An efficient CSI feedback scheme for dual-polarized massive MIMO," *IEEE Access*, vol. 6, pp. 23 420–23 430, 2018.

[8] X. Su, P. Nkurunziza, J. Gu, A. Castiglione, and C. Choi, "Inter-beam interference cancellation and physical layer security constraints by 3D polarized beamforming in power domain NOMA systems," *IEEE Trans. Sust. Comp.*, pp. 1–1, 2018.

[9] A. Adhikary, J. Nam, J. Ahn, and G. Caire, "Joint spatial division and multiplexing - The large-scale array regime," *IEEE Trans. Inf. Theory*, vol. 59, no. 10, pp. 6441–6463, Oct. 2013.

[10] H. A. David and H. N. Nagaraja, *Order Statistics*, 3rd ed. Wiley Series in Probability and Statistics, Aug. 2003.

[11] M. Abramowitz and I. Stegun, *Handbook of Mathematical Functions, With Formulas, Graphs, and Mathematical Tables*, 10th ed., ser. 55. USA: National Bureau of Standards, 1972.

[12] I. S. Gradshteyn and I. M. Ryzhik, *Table of Integrals, Series, and Products*, 7th ed., D. Zwillinger and V. H. Moll, Eds. Academic Press, 2007.